Letter

A Bioluminescent Turn-On Probe for Sensing Hypochlorite in Vitro and in Tumors

Peiyao Chen, Zhen Zheng, Yunxia Zhu, Yu Dong, Fuqiang Wang, and Gaolin Liang

Anal. Chem., **Just Accepted Manuscript** • Publication Date (Web): 09 May 2017

A Bioluminescent Turn-On Probe for Sensing Hypochlorite in Vitro and in Tumors

Peiyao Chen,[†] Zhen Zheng,[†] Yunxia Zhu,[‡] Yu Dong,[†] Fuqiang Wang,*[,†,‡] and Gaolin Liang*[,†]

[†]CAS Key Laboratory of Soft Matter Chemistry, Department of Chemistry, University of Science and Technology of China, Hefei, Anhui 230026, China.

[‡]Analysis Center, Nanjing Medical University, Nanjing, Jiangsu 210093, China.

ABSTRACT: Hypochlorite (ClO^-) is one of the most important reactive oxygen species but using a BL probe for its selective detection (or imaging) still remains challenging. Herein, we report a latent BL probe benzoylhydrazine luciferin (**1**) for highly selective detection of ClO^- *in vitro* and imaging ClO^- in living cells and tumors. *In vitro* tests indicated that **1** could be applied for highly selective detection of ClO^- within the range of 0-62.5 μM with a limit of detection of 0.705 μM. Using these unique features of **1**, we successfully applied it to image ClO^- in living cells and tumors. We envision that probe **1** might be applied to elucidate the biological roles of ClO^- in wider physiological and pathological processes in the near future.

Hypochlorite (ClO^-) is one of the most important reactive oxygen species (ROS),[1-3] which plays an important role in sustaining human innate immunity during microbial invasion.[4] Endogenous ClO^- is generated by hydrogen peroxide (H_2O_2) reacting with chloride ions (Cl^-), catalyzed by heme enzyme myeloperoxidase (MPO).[5,6] Abnormal levels of hypochlorite are reported to associate with certain diseases such as cardiovascular diseases, neuron degeneration, lung injury, atherosclerosis, arthritis, and cancer.[7-12] Thus, it is of great importance to detect or image ClO^- in cells or *in vivo*. To date, numerous fluorescence probes have been reported for the detection (or imaging) of ClO^-.[13-17] However, most of the fluorescent probes suffer from low photostability of photobleaching or autofluorescence interference from the detecting samples.

Bioluminescent imaging (BLI) is a reliable, sensitive, non-invasive imaging technique which has been widely used in imaging a myriad of life processes such as cell proliferation and migration, gene expression, and enzyme activities.[18-24] Among the approximate 30 known bioluminescence (BL) systems, the firefly luciferase-luciferin system is the most widely used one.[25] In this BL system, in the presence of adenosine triphosphate (ATP), oxygen and magnesium ions (Mg^{2+}), firefly luciferase (fLuc) catalyzes a two-step oxidation of luciferin to emit a visible (yellow to green) photon.[26-29] Notably, the generated bioluminescent photons can even penetrate the tissues of intact rodents, rendering BLI very suitable for *in vivo* imaging.[30,31] Moreover, compared with fluorescence imaging, BLI does not require external excitation and therefore possesses higher signal-to-noise ratios. To date, a variety of BL probes have been developed for the detection (or monitoring) of important analytes.[32-36] In 2015, Kojima *et al.* reported a sensitive bioluminogenic probe for *in vivo* imaging the activity of highly reactive oxygen species (hROS) including ClO^-.[37] Nevertheless, this probe could not differentiate ClO^- from other hROS. Thus, it still remains chanlleging to develop a bioluminescence probe for the selective detection of ClO^-.

Herein, we report a BL turn-on probe for *in vitro* selective detection of ClO^- and *in vivo* imaging of ClO^- in tumors. As we know, ClO^- is able to oxidize dibenzoylhydrazine into water-unstable dibenzoyl diimide.[38] Thus, as outlined in Scheme 1, we rationally designed a latent BL probe benzoylhydrazine luciferin (**1**) with the carboxyl acid group of whose D-luciferin motif being caged by benzoylhydrazine. Probe **1** itself is not the substrate for fLuc. However, upon ClO^- oxidation and follow-up hydrolysis in physiological condition, probe **1** yields the active substrate D-luciferin for luciferase to generate a light readout (Scheme 1).

Scheme 1. Schematic illustration of ClO^- oxidation of 1 to yield D-luciferin for bioluminescence generation.

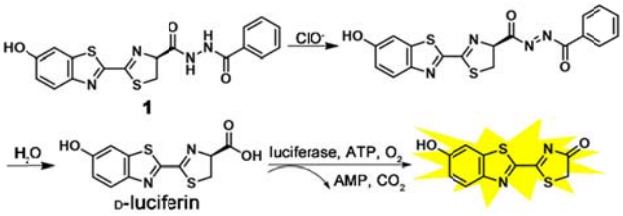

We began the study with the synthesis and characterization of probe **1** (Scheme S1, Figure S1-S3). Then we used D-luciferin to screen out an appropriate fLuc concentration to study the response of probe **1** toward ClO^-. As shown in Figure S4, the BL intensity of D-luciferin at fLuc concentration of 0.1 mg/mL was 5.3 folds of that at fLuc concentration of 0.05 mg/mL. We thus choose 0.1 mg/mL fLuc to conduct the following *in vitro* experiment. As expected, in the absence of ClO^-, almost no BL signal was generated by 1 mM **1** after being incubated with 0.1 mg/mL fLuc and 1 mM ATP in phosphate buffer (0.2 M, pH 7.4) (Figure 1A). However, addition of 70-fold ClO^- to 1 mM **1** solution resulted in a significant increase of BL intensity (a 58-fold increase at 560 nm, Figure 1A) under the same condition. This result suggested that free D-luciferin, which responds for the BL generation, was yielded from ClO^- oxidation of **1**, as we proposed in Scheme 1.

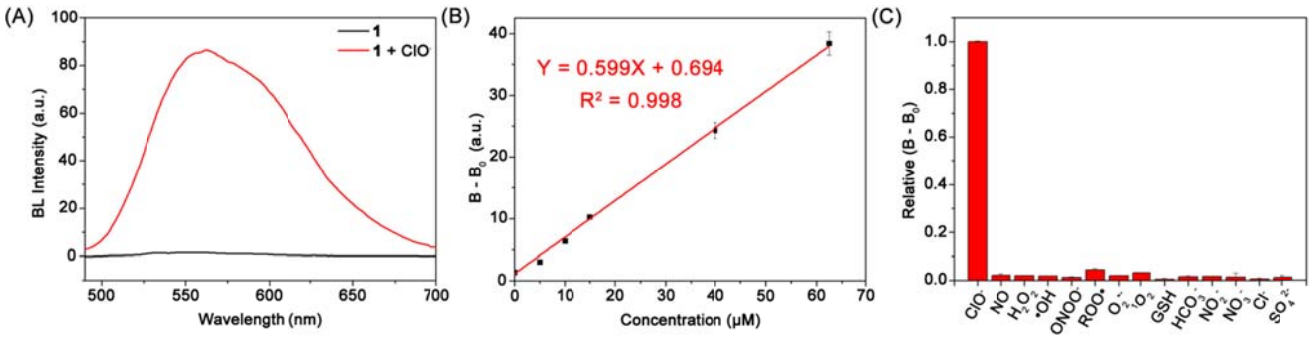

Figure 1. (A) Bioluminescent wavelength scan for 1 mM **1** and 0.1 mg/mL fLuc in the presence (red) or absence (black) of 70 mM ClO^- in phosphate buffer (0.2 M, pH 7.4). (B) Fitted calibration curve for BL intensity of 25 μM **1** at 560 nm with ClO^- concentration in the linear region of 0-62.5 μM. (C) Selectivity studies of **1**: Selectivity of **1** at 25 μM in the presence of 25 μM ClO^- or 100 μM NO, H_2O_2, hydroxyl radical (•OH), peroxynitrite ($ONOO^-$), alkylperoxyl radical (ROO•), superoxide ($O_2^{\bullet-}$), singlet oxygen ($^1O_2$), glutathione (GSH), HCO_3^-, NO_2^-, NO_3^-, Cl^-, or SO_4^{2-} respectively. The experiments were performed in triplicate. Error bars represent relative standard deviations (RSD) of three independent experiments which are 1.1×10^{-3}, 2.3×10^{-3}, 6.9×10^{-3}, 4.0×10^{-5}, 1.3×10^{-3}, 3.8×10^{-3}, 4.2×10^{-3}, 5.2×10^{-4}, 0.018, 4.4×10^{-3}, 8.2×10^{-3}, respectively. Emission: 560 nm.

High performance liquid chromatography (HPLC) analysis clearly indicated that, about 75.4% of **1** was converted to D-luciferin under this condition (Figure S5). After validation of the feasibility of **1** for ClO^- detection, a linear relationship ($Y = 0.599X + 0.694$, $R^2 = 0.998$) between the BL enhancement (i.e., B - B_0) of 25 μM **1** at 560 nm and ClO^- concentration was obtained over the range of 0-62.5 μM (Figure 1B). The limit of detection (LOD) of ClO^- of this assay was calculated to be 0.705 μM according to the general 3σ method (3σ/s),[39] comparable to those of reported methods (Table S1).

Selectivity is one important parameter to evaluate the performance of a new probe. Particularly, for a new probe which is intentionally designed for biomedical applications, its highly selective response to the target over other possible competitive species is a must. Therefore, we screened a wide array of the potential competitive species such as intracellular reactive oxygen and nitrogen species (ROS/RNS) (e.g., NO, H_2O_2, •OH, $ONOO^-$, ROO•, $O_2^{\bullet-}$, and $^1O_2$), intracellular abundant biomolecules (e.g., GSH) and common anions (e.g., HCO_3^-, NO_2^-, NO_3^-, Cl^-, and SO_4^{2-}) to study the selectivity of probe **1** by comparing its B - B_0 value induced by ClO^- over those of the selected species in the presence of fLuc. As shown in Figure 1C, only 100 μM ROO• and $^1O_2$ showed weak bioluminescence after addition to 25 μM **1**, which was almost negligible compared to that induced by ClO^- (BL enhancement by ClO^- was 23-182 folds of those induced by other species). Therefore, we concluded that probe **1** has excellent selectivity toward ClO^- over other testing species.

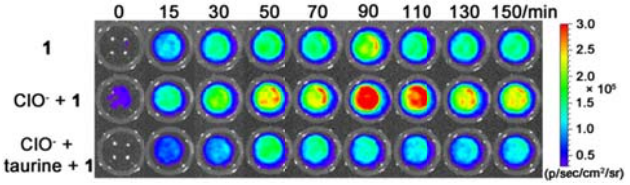

Figure 2. Time-course bioluminescence images of fLuc-transfected MDA-MB-231 cells incubated with 50 μM **1** (top row), pre-incubated with 5 μM exogenous ClO^- and then with 50 μM **1** (middle row), pre-incubated with 5 μM exogenous ClO^- followed by 25 mg/mL ClO^- scavenger taurine and then with 50 μM **1** (bottom row) acquired at 0, 15, 30, 50, 70, 90, 110, 130 and 150 min in serum-free culture medium at 37 °C.

With its good *in vitro* property, probe **1** was subsequently applied for BL imaging ClO^- in living cells. Before that, cytotoxicity of **1** and ClO^- was evaluated on MDA-MB-231 cells (non-luciferase transfected) with 3-(4,5-dimethylthiazol-2-yl) 2,5 diphenyltetrazplium bromide (MTT) assay. As shown in Figure S6, 90.0% of the cells survived after 24 h incubation with 100 μM **1**, suggesting that probe **1** under 100 μM is safe for live cell imaging. For ClO^-, 95% of the cells survived after 4 h incubation with 20 μM ClO^- (Figure S7), suggesting that ClO^- concentration under 20 μM is safe for live cell imaging. In this work, we chose **1** at 50 μM and ClO^- at 5 μM to conduct the following cell imaging study. FLuc–transfected MDA-MB-231 cells were pre-incubated with or without 5 μM ClO^- in serum-free culture medium at 37 °C for 30 min, and washed with phosphate buffered saline (PBS) for three times to remove extracellular ClO^-. Then the cells were placed in the 96-well plate at 1×10^6 cells/well. BL signals generated by the cells were recorded with a small animal imaging system in a real-time manner. Generally, as shown in Figure 2, after the addition of probe **1** to each well, the BL signals gradually increased to the maximum at around 90 min, followed by a decrease, and then maintained at comparable values over the observation window (Figure S8). To be specific, the brightest BL signal was observed from the cells pre-incubated with ClO^- (middle row in Figure 2), suggesting that probe **1** has good cell permeability, and can be oxidized by ClO^- to yield D-luciferin inside cells. However, when the cells were incubated with 25 mg/mL ClO^- scavenger taurine[40] for 5 min before the addition of **1** to the ClO^- pre-incubation cells, their BL signal (bottom row in Figure 2) was significantly decreased compared to that of ClO^--treated cells. This demonstrated that ClO^- could trigger **1** to release of D-luciferin for BL generation in cells. For the cells without pre-incubation of ClO^-, weak BL signal could be detected (top row in Figure 2). This could be explained that the intracellular proteases hydrolyzed the amide bond of **1** to yield D-luciferin to generate the weak BL because MDA-MB-231 cells themselves do not generate ClO^-. HPLC analysis indicated that, after the MDA-MB-231 cells (non-luciferase transfected) were incubated with 200 μM **1** for 30 min, 15.4% of uptaken **1** was proteolysed to yield D-luciferin inside cells (Figure S9). For the ClO^--pretreated cells, incubation with probe **1** resulted in a three-time increased amount of D-luciferin inside cells, compared with those cells without ClO^- treatment (Figure S9). This further comfirmed that most of the intracellular D-luciferin was generated by **1** that reacted with ClO^- for the BL

augmentation. We also conducted cell imaging experiment with the cells pre-incubated with **1** before ClO^- addition. As shown in Figure S10, the brightest BL signal was also observed from the cells with ClO^- addition. However, the BL signal increased to the maximum much quicker (15 min after ClO^- addition) and then decreased gradually (Figure S11). This could be explained that, upon the addition of ClO^-, probe **1** was turned into D-luciferin in the medium, resulting in similar cell imaging pattern to that of cells directly incubated with D-luciferin.[32] The above results suggest that probe **1** is suitable for BLI of ClO^- in living cells.

We then applied **1** for BLI of ClO^- in living animals. The nude mice, xenografted with fLuc-transfected MDA-MB-231 tumor in the right thigh for each, were randomly divided into three groups (one group for the injection of ClO^- followed by injection of **1** as the experimental group, one group for the injection of **1** only and one group for the successive injections of ClO^-, taurine, and **1** as the two control groups). BL signal generated from the tumors in the nude mice was then recorded in real-time by a small animal imaging system. As shown in Figure 3, even without ClO^- injection, tumors of **1**-injected mice also exhibited weak BL signal (top row in Figure 3). This could be explained that small amount of **1** was hydrolyzed by intracellular proteases of tumor cells to yield D-luciferin for BL generation. However, within the observation time (i.e., 20-220 min), the BL intensity of the experimental group remained the highest (middle row in Figure 3). It increased to the peak at 70 min, and then decreased slowly thereafter (Figure S12), suggesting that, under ClO^- oxidation, most of **1** yielded D-luciferin for the strong BL. ClO^--scavenging control experiment indicated that the taurine-treated mice had obviously lower BL intensity than that of the experimental group (bottom row in Figure 3). This further affirmed that above strong BL from experimental group was resulted from ClO^- oxidation of **1** to yield D-luciferin. These *in vivo* results demonstrated that probe **1** could be applied for imaging ClO^- in tumors of living animals.

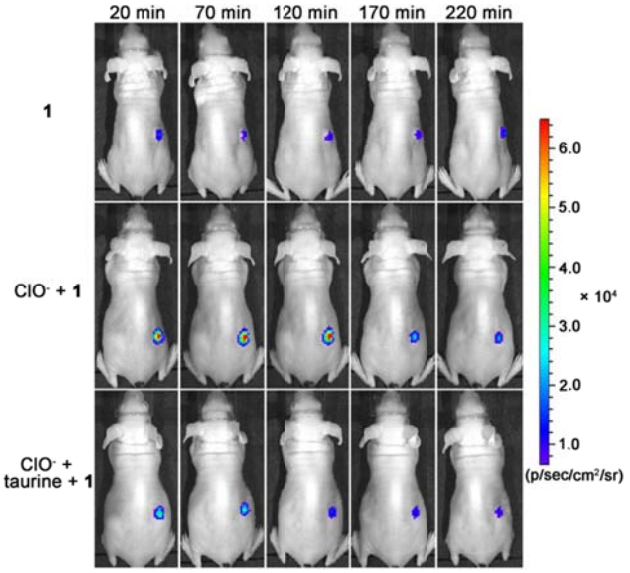

Figure 3. Time-course bioluminescence imaging of nude mice xenografted with fLuc-transfected MDA-MB-231 tumors after intraperitoneal injection of 100 μL **1** at 2.5 mM (top row), 100 μL ClO^- at 1 mM followed by 100 μL **1** at 2.5 mM 5 min later (middle row), or 100 μL ClO^- at 1 mM followed by 100 μL taurine at 50 mg/mL 5 min later and 100 μL **1** at 2.5 mM 5 min later (bottom row) in PBS at 20, 70, 120, 170, and 220 min.

In summary, we have successfully developed a latent bioluminescent probe **1** for highly selective detection of ClO^- *in vitro* and imaging ClO^- in tumors of living mice. Upon ClO^- oxidation and the follow-up hydrolysis, **1** was converted to D-luciferin for BL generation in the presence of fLuc. This property of **1** was successfully applied for highly selective detection of ClO^- within 0-62.5 μM and a LOD of 0.705 μM *in vitro*. The feasibility of this assay for imaging ClO^- in living cells and in tumors was also validated. With these unique features of **1**, we envision that it might be applied to elucidate the biological roles of ClO^- in wider physiological and pathological processes in the near future.

ASSOCIATED CONTENT

Supporting Information

General methods; Syntheses and characterizations of **1**; Supporting scheme, figures, and tables (Scheme S1, Figure S1-S12, and Table S1-S3). This material is available free of charge via the Internet at http://pubs.acs.org.

AUTHOR INFORMATION

Corresponding Authors

*E-mail: wangfq@njmu.edu.cn

*E-mail: gliang@ustc.edu.cn

Notes

The authors declare no competing financial interests.

ACKNOWLEDGMENT

This work was supported by Collaborative Innovation Center of Suzhou Nano Science and Technology, Hefei Science Center CAS (2016HSC-IU010), Ministry of Science and Technology of China (2016YFA0400904), and the National Natural Science Foundation of China (Grants 21675145 and U1532144).

REFERENCES

(1) McCord, J. M. *Science* **1974**, *185*, 529-531.
(2) D'Autréaux, B.; Toledano, M. B. *Nat. Rev. Mol. Cell Biol.* **2007**, *8*, 813-824.
(3) Mittal, M.; Siddiqui, M. R.; Tran, K.; Reddy, S. P.; Malik, A. B. *Antioxid. Redox Signal.* **2014**, *20*, 1126-1167.
(4) Hidalgo, E.; Bartolome, R.; Dominguez, C. *Chem.-Biol. Interact.* **2002**, *139*, 265-282.
(5) Goiffon, R. J.; Martinez, S. C.; Piwnica-Worms, D. *Nat. Commun.* **2015**, *6*, 6271.
(6) Harrison, J.; Schultz, J. *J. Biol. Chem.* **1976**, *251*, 1371-1374.
(7) Sugiyama, S.; Okada, Y.; Sukhova, G. K.; Virmani, R.; Heinecke, J. W.; Libby, P. *J. Pathol.* **2001**, *158*, 879-891.
(8) Yap, Y. W.; Whiteman, M.; Cheung, N. S. *Cell. Signal.* **2007**, *19*, 219-228.
(9) Hammerschmidt, S.; Buchler, N.; Wahn, H. *Chest* **2002**, *121*, 573-581.
(10) Daugherty, A.; Dunn, J. L.; Rateri, D. L.; Heinecke, J. W. *J. Clin. Invest.* **1994**, *94*, 437-444.

(11) Wu, S. M.; Pizzo, S. V. *Arch. Biochem. Biophys.* **2001**, *391*, 119-126.
(12) Weitzman, S. A.; Gordon, L. *Blood* **1990**, *76*, 655-663.
(13) Shepherd, J.; Hilderbrand, S. A.; Waterman, P.; Heinecke, J. W.; Weissleder, R.; Libby, P. *Chem. Biol.* **2007**, *14*, 1221-1231.
(14) Chen, T.; Hu, Y.; Cen, Y.; Chu, X.; Lu, Y. *J. Am. Chem. Soc.* **2013**, *135*, 11595-11602.
(15) Goswami, S.; Das, A. K.; Manna, A.; Maity, A. K.; Saha, P.; Quah, C. K.; Fun, H.-K.; Abdel-Aziz, H. A. *Anal. Chem.* **2014**, *86*, 6315-6322.
(16) Hou, J.; Wu, M.; Li, K.; Yang, J.; Yu, K.; Xie, Y.; Yu, X. *Chem. Commun.* **2014**, *50*, 8640-8643.
(17) Wu, Y.; Wang, J.; Zeng, F.; Huang, S.; Huang, J.; Xie, H.; Yu, C.; Wu, S. *ACS Appl. Mater. Interfaces* **2016**, *8*, 1511-1519.
(18) Dragulescu-Andrasi, A.; Liang, G.; Rao, J. *Bioconjugate Chem.* **2009**, *20*, 1660-1666.
(19) Jacobson, G. B.; Shinde, R.; Contag, C. H.; Zare, R. N. *Angew. Chem. Int. Ed.* **2008**, 47, 7880-7882.
(20) Yuan, Y.; Wang, F.; Tang, W.; Ding, Z.; Wang, L.; Liang, L.; Zheng, Z.; Zhang, H.; Liang, G. *ACS Nano* **2016**, *10*, 7147-7153.
(21) Yang, Y.; Shao, Q.; Deng, R.; Wang, C.; Teng, X.; Cheng, K.; Cheng, Z.; Huang, L.; Liu, Z.; Liu, X. Xing, B. *Angew. Chem. Int. Ed.* **2012**, *51*, 3125-3129.
(22) Zheng, Z.; Li, G.; Wu, C.; Zhang, M.; Zhao, Y.; Liang, G. *Chem. Commun.* **2017**, *53*, 3567-3570.
(23) Evans, M. S.; Chaurette, J. P.; Adams Jr, S. T.; Reddy, G. R.; Paley, M. A.; Aronin, N.; Prescher, J. A.; Miller, S. C. *Nat. Methods* **2014**, *11*, 393-395.
(24) Adams, S. T.; Mofford, D. M.; Reddy, G.; Miller, S. C. *Angew. Chem. Int. Ed.* **2016**, *55*, 4943-4946.
(25) Kaskova, Z. M.; Tsarkova, A. S.; Yampolsky, I. V. *Chem. Soc. Rev.* **2016**, *45*, 6048-6077.
(26) Li, J.; Chen, L.; Du, L.; Li, M. *Chem. Soc. Rev.* **2013**, *42*, 662-676.
(27) Marques, S. M.; Esteves da Silva, J. C. *IUBMB Life* **2009**, *61*, 6-17.
(28) McCutcheon, D. C.; Paley, M. A.; Steinhardt, R. C.; Prescher, J. A. *J. Am. Chem. Soc.* **2012**, *134*, 7604-7607.
(29) Conley, N. R.; Dragulescu‐Andrasi, A.; Rao, J.; Moerner, W. *Angew. Chem. Int. Ed.* **2012**, *51*, 3350-3353.
(30) Van de Bittner, G. C.; Bertozzi, C. R.; Chang, C. J. *J. Am. Chem. Soc.* **2013**, *135*, 1783-1795.
(31) Heffern, M. C.; Park, H. M.; Au-Yeung, H. Y.; Van de Bittner, G. C.; Ackerman, C. M.; Stahl, A.; Chang, C. J. *Proc. Natl. Acad. Sci. U. S. A.* **2016**, *113*, 14219-14224.
(32) Zheng, Z.; Wang, L.; Tang, W.; Chen, P.; Zhu, H.; Yuan, Y.; Li, G.; Zhang, H.; Liang, G. *Biosens. Bioelectron.* **2016**, *83*, 200-204.
(33) Takakura, H.; Kojima, R.; Kamiya, M.; Kobayashi, E.; Komatsu, T.; Ueno, T.; Terai, T.; Hanaoka, K.; Nagano, T.; Urano, Y. *J. Am. Chem. Soc.* **2015**, *137*, 4010-4013.
(34) Wu, W.; Li, J.; Chen, L.; Ma, Z.; Zhang, W.; Liu, Z.; Cheng, Y.; Du, L.; Li, M. *Anal. Chem.* **2014**, *86*, 9800-9806.
(35) Cohen, A. S.; Dubikovskaya, E. A.; Rush, J. S.; Bertozzi, C. R. *J. Am. Chem. Soc.* **2010**, *132*, 8563-8565.
(36) Jiang, T.; Ke, B.; Chen, H.; Wang, W.; Du, L.; Yang, K.; Li, M. *Anal. Chem.* **2016**, *88*, 7462-7465.
(37) Kojima, R.; Takakura, H.; Kamiya, M.; Kobayashi, E.; Komatsu, T.; Ueno, T.; Terai, T.; Hanaoka, K.; Nagano, T.; Urano, Y. *Angew. Chem. Int. Ed.* **2015**, *54*, 14768-14771.
(38) Chen, X.; Wang, X.; Wang, S.; Shi, W.; Wang, K.; Ma, H. *Chem.-Eur. J.* **2008**, *14*, 4719-4724.
(39) Ogren, P. J.; Meetze, A.; Duer, W. C. *J. Anal. Toxicol.* **2009**, *33*, 129-142.
(40) Weiss, S. J.; Klein, R.; Slivka, A.; Wei, M. *J. Clin. Invest.* **1982**, *70*, 598-607.

For TOC only